Chaos
An Interdisciplinary Journal of Nonlinear Science

RESEARCH ARTICLE | JULY 17 2023

Synchronization and stability analysis of an exponentially diverging solution in a mathematical model of asymmetrically interacting agents

Yusuke Kato ; Hiroshi Kori

Chaos 33, 073133 (2023)
https://doi.org/10.1063/5.0151174

Synchronization and stability analysis of an exponentially diverging solution in a mathematical model of asymmetrically interacting agents

Cite as: Chaos 33, 073133 (2023); doi: 10.1063/5.0151174
Submitted: 19 March 2023 · Accepted: 26 June 2023 ·
Published Online: 17 July 2023

Yusuke Kato[a] and Hiroshi Kori

AFFILIATIONS

Department of Complexity Science and Engineering, Graduate School of Frontier Sciences, The University of Tokyo, Kashiwa, Chiba 277-8561, Japan

[a]**Author to whom correspondence should be addressed:** yuukato@g.ecc.u-tokyo.ac.jp

ABSTRACT

This study deals with an existing mathematical model of asymmetrically interacting agents. We analyze the following two previously unfocused features of the model: (i) synchronization of growth rates and (ii) initial value dependence of damped oscillation. By applying the techniques of variable transformation and timescale separation, we perform the stability analysis of a diverging solution. We find that (i) all growth rates synchronize to the same value that is as small as the smallest growth rate and (ii) oscillatory dynamics appear if the initial value of the slowest-growing agent is sufficiently small. Furthermore, our analytical method proposes a way to apply stability analysis to an exponentially diverging solution, which we believe is also a contribution of this study. Although the employed model is originally proposed as a model of infectious disease, we do not discuss its biological relevance but merely focus on the technical aspects.

Nonlinear dynamical systems exhibit a wide variety of behaviors, e.g., hysteresis, limit cycle, synchronization, and chaos. Elucidating these nonlinear phenomena is an important issue, as well as the development of new analytical methods. Here, we analyze an existing nonlinear system and clarify the two properties that were not previously focused on, i.e., synchronization of growth rates and initial value dependence of damped oscillation. In the analysis, we propose a novel method to perform the linear stability analysis of an exponentially diverging solution, which is expected to help further investigate the nonlinear dynamics.

I. INTRODUCTION

It is widely known that nonlinear systems show various complex behaviors.[1] Those behaviors are extensively studied since the late 19th century: the discovery of chaotic dynamics on a strange attractor[2] and the analysis of synchronization transition[3,4] are examples of such theoretical research. Nonlinear dynamical systems are also used to describe various phenomena in nature and society, especially in population dynamics.[5] For example, the outbreak of a certain insect is explained as hysteresis,[6] varying prey–predator populations are described as periodic orbits,[7,8] and synchronous firefly flashing[9] or frog calls[10] are modeled with coupled nonlinear oscillators. Therefore, it is important to establish theoretical frameworks for nonlinear phenomena, which would provide deeper insight into complex phenomena and contribute to broadening applications. In addition, since most of the nonlinear differential equations cannot be explicitly solved, the development of novel analytical techniques is crucial to further study the nonlinear system.

In the present paper, we focus on peculiar dynamical behavior observed in the model proposed in Ref. 11 The model is described by a $2n$-dimensional dynamical system. The model elements are divided into two groups of n agents [i.e., v_i and x_i in Eq. (1)] and these groups interact with each other asymmetrically.

In the original paper, the authors investigated the dynamics of this model in both analytical and numerical ways.[11] However, there are several open questions in their study. First, they did not

analyze the following two features of numerical results: the amount of agents in one group [i.e., v_i in Eq. (1)] (i) initially oscillates and then decreases to a very low level and (ii) increases extremely slowly despite the existence of fast-growing agents. Second, the analysis in the original paper was valid only under the assumption that the dynamics of agents in the other group [i.e., x_i in Eq. (1)] are sufficiently fast.

We are particularly concerned with the two features observed numerically because they are considered to reflect the nonlinearity of the model. In addition, we expect that removing the assumption of fast dynamics is necessary to analyze the initial oscillatory behavior. Therefore, in this study, we aim to clarify the mechanisms of initial oscillation and the extremely slow growth by analyzing this model under more general conditions; i.e., without assuming the fast dynamics.

The summary of our results is as follows: in the case when $n = 2$, numerical simulations suggest that the initial oscillation and the following slow growth of agents in one group [i.e., v_i in Eq. (1)] appear if one agent has a considerably lower growth rate than the other. We perform the existence and linear stability analysis without assuming that the dynamics of agents in the other group [i.e., x_i in Eq. (1)] are sufficiently fast. We determine that an oscillation occurs if the initial value of the slow-growing agent is sufficiently small. Next, we generalize these results for the case when $n \geq 3$ and one agent has a considerably lower growth rate ε than the others. In particular, we prove that (i) all growth rates synchronize to the same value of $O(\varepsilon)$ if the parameters satisfy a few conditions and (ii) damped oscillation exists if the initial value of the slowest-growing mutant is sufficiently small.

Our work is a theoretical study that reveals nontrivial and previously unfocused features of a nonlinear dynamical system of asymmetrically interacting agents. This study is also novel in that we perform the stability analysis of the dynamics that oscillate and diverge, compared to the previous works that analyze the stability of equilibrium solutions in mathematical models regarding population dynamics.[12–15]

II. MATHEMATICAL MODEL AND NONDIMENSIONALIZATION

Our model is based on the one proposed in Ref. 11. The dynamics of $2n$ agents, which are originally introduced as n viral mutants and corresponding immune cells,[11] are described by the following dynamical system:

$$\dot{v}_i = \frac{dv_i}{dt} = v_i(r_i - p_i x_i), \tag{1a}$$

$$\dot{x}_i = \frac{dx_i}{dt} = kv_i - ux_i \sum_{j=1}^{n} v_j, \tag{1b}$$

where v_i denotes the amount of mutant virus i, x_i is the quantity of strain-specific immune cells attacking the virus i, and n represents the number of viral mutant strains ($1 \leq i \leq n$). The parameter r_i is the growth rate of virus i, p_i represents the strength of the immune attack on virus i, k is the activation rate of immune cells, and u represents the strength of the viral attack on immune cells. Note the asymmetric interaction between the virus and immune cells; even though each strain of immune cells x_i is specific to virus i, virus i can attack all strains of immune cells. The parameters r_i, p_i, k, and u are assumed to be positive constants.

We introduce dimensionless quantities $\alpha_i := \frac{r_i}{r_1}$, $\tilde{v}_i := \frac{u}{r_1} v_i$, $\tilde{x}_i := \frac{p_i}{r_i} x_i$, $\tau := r_1 t$, and $q_i := \frac{p_i k}{r_i u}$. By renaming $\tilde{v}_i \to v_i$, $\tilde{x}_i \to x_i$, and $\tau \to t$, we transform Eq. (1) into the following dimensionless system:

$$\dot{v}_i = \alpha_i v_i(1 - x_i), \tag{2a}$$

$$\dot{x}_i = v_i \left(q_i - x_i \frac{\sum_{j=1}^{n} v_j}{v_i} \right). \tag{2b}$$

The parameter α_i is the ratio of growth rates among viral mutants and q_i represents the immunological strength of x_i compared with the virulence of v_i. We assume $0 < \alpha_n \leq \cdots \leq \alpha_2 \leq \alpha_1 = 1$ without loss of generality.

III. THE CASE WHEN $n = 1$

When there is only one viral mutant (i.e., $n = 1$), our model is given by

$$\dot{v} = v(1 - x), \tag{3a}$$

$$\dot{x} = v(q - x). \tag{3b}$$

Figure 1 presents the simulation results, where we assume that the initial value of x is zero [i.e., $x(0) = 0$] because virus-specific immunity has not been prepared at the beginning of infection. Then, the viral dynamics are classified into the following two types: (i) for $q < 1$, the viral load continues to increase [Figs. 1(a) and 1(b)] and (ii) for $q > 1$, the viral load initially increases and subsequently decreases, eventually converging to zero [Figs. 1(c) and 1(d)].

We investigate the mechanism of the obtained dynamics in Fig. 1. Obviously, $(v, x) = (0, x)$ with arbitrary $x \in \mathbf{R}$ is the fixed point of the system (3). By performing the linear stability analysis, the Jacobian matrix at this fixed point is

$$\begin{pmatrix} 1 - x & -v \\ q - x & -v \end{pmatrix}\Bigg|_{(v,x)=(0,x)} = \begin{pmatrix} 1 - x & 0 \\ q - x & 0 \end{pmatrix}, \tag{4}$$

and its eigenvalues are 0 and $1 - x$. The 0 eigenvalue corresponds to the eigenvector ${}^t(0, 1)$, which is parallel to the line $v = 0$ (the set of fixed points). Thus, we expect that the fixed point $(0, x)$ is unstable if $x < 1$ and Lyapunov stable if $x > 1$, which agrees with the flows in the phase planes [Figs. 1(b) and 1(d)]. This is why the viral load with the initial conditions $(v(0), x(0)) = (0.01, 0)$ (i.e., starting from the neighborhood of the unstable fixed point) diverges in Fig. 1(a) and initially increases in Fig. 1(c). As the viral load v increases, the immune cell x that starts from $x = 0$ also increases [see Eq. (3b)]. However, since the line $x = q$ in the phase plane is the invariant subspace, we find that the immune cell x cannot exceed q (i.e., the other solution cannot intersect with the line $x = q$) according to the uniqueness of the solution of ordinary differential equations. Therefore, if $q < 1$, the immune cell x is always smaller than 1 and the viral load v continues to increase [Fig. 1(a)], and if $q > 1$, the immune

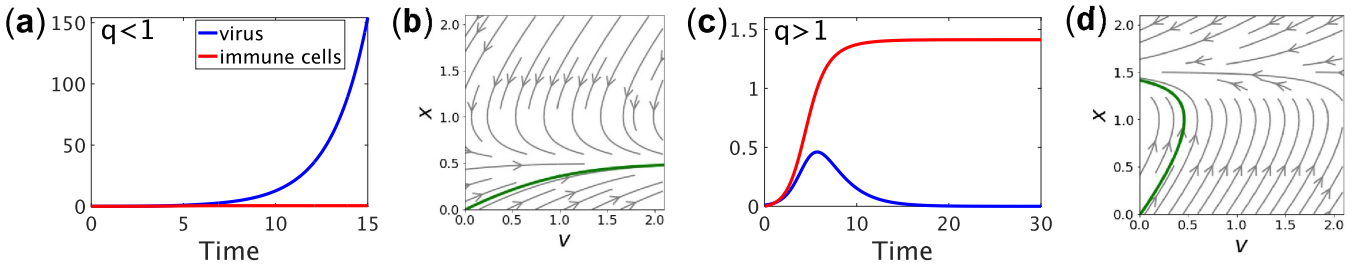

FIG. 1. The numerical simulations for one viral mutant case. Panels (a) and (c) represent the time course of the virus and immune cells, using the same initial conditions $v(0) = 0.01$ and $x(0) = 0$. Panels (b) and (d) display the phase planes where the green line in each phase plane is the trajectory that starts from $(v(0), x(0)) = (0.01, 0)$. (a) and (b) When $q < 1$, the total viral load continues to increase (we set $q = 0.5$). (c) and (d) When $q > 1$, the total viral load decreases after the initial peak and converges to zero (we set $q = 1.5$).

cell x can exceed 1 as v increases and then v decreases [i.e., $\dot{v} < 0$ in Eq. (3a)] while x approaches to a fixed point x^* that satisfies $x^* > 1$ [Fig. 1(c)].

Based on Fig. 1 and the above discussion, we conclude that the initial oscillation and the following slow viral growth observed in the numerical simulation of the previous study[11] cannot be reproduced in the case of one viral mutant.

IV. THE CASE WHEN $n = 2$

For $n = 2$, our model is given as

$$\dot{v}_1 = v_1(1 - x_1), \tag{5a}$$

$$\dot{v}_2 = \alpha_2 v_2(1 - x_2), \tag{5b}$$

$$\dot{x}_1 = v_1\left[q_1 - x_1\left(1 + \frac{v_2}{v_1}\right)\right], \tag{5c}$$

$$\dot{x}_2 = v_2\left[q_2 - x_2\left(1 + \frac{v_1}{v_2}\right)\right]. \tag{5d}$$

A. Simulation results

Figure 2 demonstrates the simulation results. In Figs. 2(a) and 2(b), we consider the situation in which two viral mutants have similar replication rates and the immunity is strong enough to eradicate the virus. Next, we weaken the immunity, or decrease q_i, so that the viral load diverges [Figs. 2(c) and 2(d)]. Finally, we notably reduce α_2 to simulate a slow-replicating mutant [Figs. 2(e) and 2(f)]. Throughout these simulations, we use the same initial conditions [$v_1(0) = v_2(0) = 0.01$ and $x_1(0) = x_2(0) = 0$] because it is natural to assume that the amount of virus is very low and virus-specific immunity has not been established at the beginning of the infection.

The dynamics observed in Figs. 2(a)–2(d) are qualitatively the same as those obtained in Sec. III. In contrast, Figs. 2(e) and 2(f) demonstrate a new pattern with two components, namely, damped oscillation and slow exponential viral growth, which was previously observed but not analyzed.[11] We are going to clarify the origin of this simulation result.

B. Analysis

We expect that the dynamics in Figs. 2(e) and 2(f) may arise when $\alpha_2 \ll 1$. Thus, we treat α_2 as a small parameter and put $\varepsilon := \alpha_2$. The other parameters are assumed to be $O(1)$.

In Figs. 2(e) and 2(f), we observe that $x_i(t)$ converges toward a nonzero constant, denoted by x_i^*, whereas v_i diverges. Based on Eq. (5), this condition is only possible when $\beta := \frac{v_2}{v_1}$ also converges toward a positive constant, represented by β^*. Assuming the convergence of β to β^*, we obtain the fixed point x_i^* in Eqs. (5c) and (5d), which is given as

$$x_1^* = \frac{q_1}{1 + \beta^*}, \quad \text{and} \quad x_2^* = \frac{q_2\beta^*}{1 + \beta^*}. \tag{6}$$

Substituting $x_i = x_i^*$ into $\dot{\beta} = \frac{v_1\dot{v}_2 - v_2\dot{v}_1}{v_1^2} = 0$, we further obtain

$$\beta^* = \frac{q_1 - 1 + \varepsilon}{1 + \varepsilon(q_2 - 1)} = q_1 - 1 + O(\varepsilon). \tag{7}$$

For sufficiently small ε, the condition $\beta^* > 0$ holds when

$$q_1 > 1. \tag{8}$$

Thus, we assume this inequality below. Substituting $x_i = x_i^*$ and $\beta = \beta^*$ into Eqs. (5a) and (5b), we obtain

$$\dot{v}_1 = \lambda v_1 \quad \text{and} \quad \dot{v}_2 = \lambda v_2,$$

where

$$\lambda = \frac{\varepsilon(q_1 + q_2 - q_1q_2)}{q_1 + \varepsilon q_2} = O(\varepsilon). \tag{9}$$

We also assume $q_1 + q_2 - q_1q_2 > 0$ so that $\lambda > 0$. Therefore, if x_i and β sufficiently approach x_i^* and β^*, respectively, v_1 and v_2 exponentially increase with the same timescale λ^{-1} of $O(\varepsilon^{-1})$. In other words, the effective replication rates of both viral mutants synchronize to the same value λ, which is as small as the slow-replicating mutant's replication rate ε.

We now perform the stability analysis of the obtained solution by invoking the notion of timescale separation. For convenience, we introduce new variables $w_i(t)$ as $w_i := v_i e^{-\lambda t}$. Then, Eq. (5) is transformed to the following four-dimensional nonautonomous system:

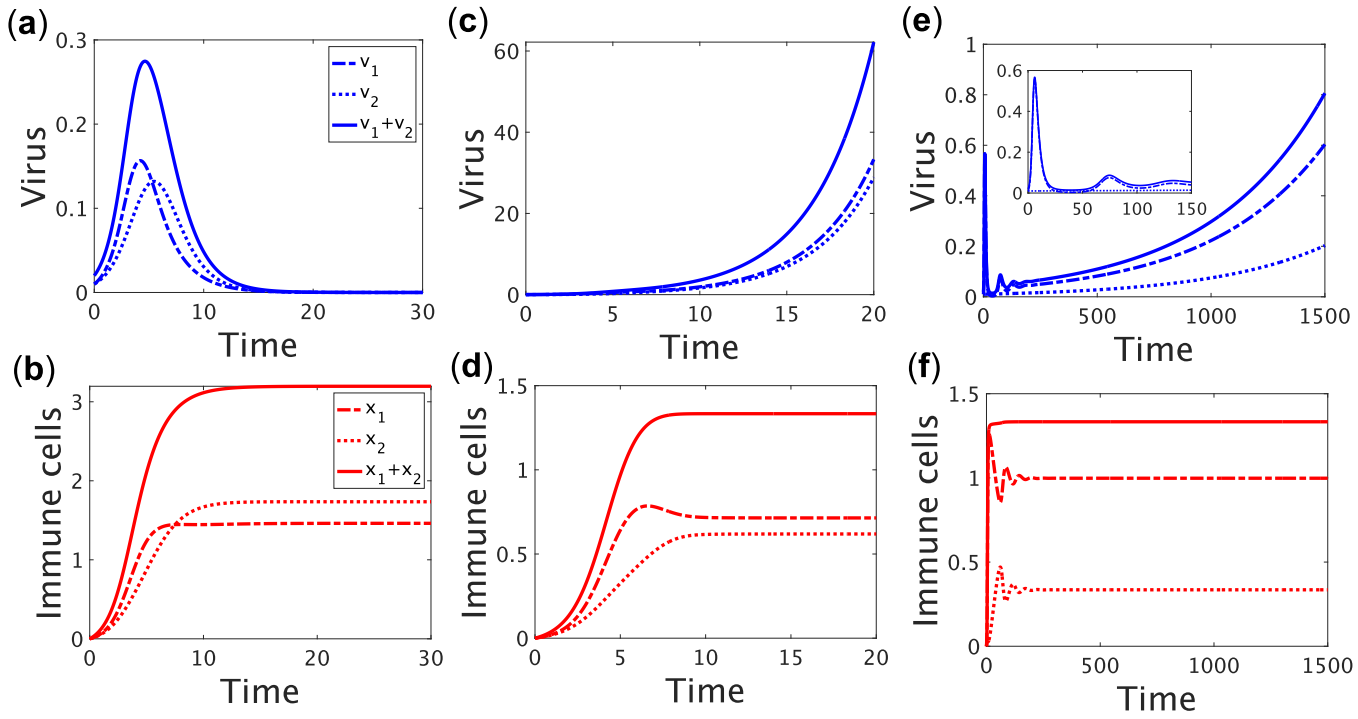

FIG. 2. Time course of the viral load (v_1, v_2) and immune cells (x_1, x_2) in various parameters. (a) and (b) Virus replicates transiently and is then eliminated from the body. (c) and (d) Virus continues to grow exponentially. (e) and (f) After initial proliferation, the viral load decreases to a low level. However, the viral load increases again and finally diverges. The parameters are as follows: $\alpha_2 = 0.75, q_1 = q_2 = 4$ for panels (a) and (b), $\alpha_2 = 0.75, q_1 = q_2 = \frac{4}{3}$ for panels (c) and (d), and $\alpha_2 = 0.003, q_1 = q_2 = \frac{4}{3}$ for panels (e) and (f) . We use the same initial conditions $v_1(0) = v_2(0) = 0.01$ and $x_1(0) = x_2(0) = 0$.

$$\dot{w}_1 = w_1(1 - \lambda - x_1), \tag{10a}$$

$$\dot{w}_2 = \varepsilon w_2 \left(1 - \frac{\lambda}{\varepsilon} - x_2\right), \tag{10b}$$

$$\dot{x}_1 = e^{\lambda t} w_1 \left[q_1 - x_1 \left(1 + \frac{w_2}{w_1}\right)\right], \tag{10c}$$

$$\dot{x}_2 = e^{\lambda t} w_2 \left[q_2 - x_2 \left(1 + \frac{w_1}{w_2}\right)\right]. \tag{10d}$$

As far as $t = O(1)$, we can safely replace $e^{\lambda t}$ in Eqs. (10c) and (10d) with 1 because $e^{\lambda t} = 1 + O(\lambda t) = 1 + O(\varepsilon)$. Moreover, w_2 is a slow variable. Thus, in a good approximation, the dynamics of w_1, x_1, and x_2 are described by the following three-dimensional autonomous subsystem:

$$\dot{w}_1 = w_1(1 - \lambda - x_1), \tag{11a}$$

$$\dot{x}_1 = w_1 \left[q_1 - x_1 \left(1 + \frac{w_2}{w_1}\right)\right], \tag{11b}$$

$$\dot{x}_2 = w_2 \left[q_2 - x_2 \left(1 + \frac{w_1}{w_2}\right)\right], \tag{11c}$$

in which w_2 is regarded as a constant. This subsystem has a nontrivial fixed point $(w_1, x_1, x_2) = (w_1^*, x_1^*, x_2^*)$, where $w_1^* = \frac{w_2}{\beta^*}$ and x_i^* are given in Eq. (6). The Jacobian matrix at this fixed point is

$$\begin{pmatrix} 0 & -w_1^* & 0 \\ q_1 - x_1^* & -(w_1^* + w_2) & 0 \\ -x_2^* & 0 & -(w_1^* + w_2) \end{pmatrix}, \tag{12}$$

and its eigenvalues are

$$-\frac{(1+\beta^*)w_2}{\beta^*} \quad \text{and} \quad \frac{-\frac{(1+\beta^*)w_2}{\beta^*} \pm \sqrt{D_0}}{2}, \tag{13}$$

where

$$D_0 = \frac{(1+\beta^*)^2 w_2^2}{(\beta^*)^2} - \frac{4q_1 w_2}{1+\beta^*}. \tag{14}$$

Regardless of the sign of D_0, all eigenvalues have negative real parts. Thus, the fixed point under consideration is asymptotically stable. We also determine that imaginary eigenvalues appear if $D_0 < 0$; i.e.,

$$0 < w_2 < \frac{4q_1(\beta^*)^2}{(1+\beta^*)^3} = \frac{4q_1(q_1 - 1 + \varepsilon)^2(1 + \varepsilon(q_2 - 1))}{(q_1 + \varepsilon q_2)^3}. \tag{15}$$

Oscillation arises in this case.

The fast variables stay in the ε-vicinity of the fixed point in the full system after the transient process because the subsystem of the

fast variables has a stable fixed point $(w_1, x_1, x_2) = (w_1^*, x_1^*, x_2^*)$. Substituting $x_2 = x_2^* + O(\varepsilon)$ into Eq. (10b) and further using Eqs. (7) and (9), we obtain $\dot{w}_2 = O(\varepsilon^2)$, which implies that $w_2(t) = w_2(0) + O(\varepsilon^2)$ for $t = O(1)$. Therefore, w_2 in inequality (15) can be regarded as $w_2(0)$ in a good approximation. Consequently, we conclude that oscillation inevitably occurs if there is a viral mutant whose replication rate is considerably smaller than the other's and its initial value is sufficiently small; i.e.,

$$v_2(0) = w_2(0) < \frac{4q_1(\beta^*)^2}{(1+\beta^*)^3}. \tag{16}$$

Moreover, both viral mutants share an effective growth rate of $\lambda = O(\varepsilon)$, namely, the slow mutant entrains the fast mutant. This synchronization underlies the emergence of the phase of low viral load.

Finally, we discuss the mechanism of the damped oscillation by considering the dynamics of system (11) qualitatively. Note that the first two equations are closed with respect to w_1 and x_1 since we regard w_2 as a constant [i.e., $w_2 \simeq w_2(0)$]. Assuming the same initial condition as in Figs. 2(e) and 2(f) (i.e., $w_1(0) = w_2(0) = 0.01$ and $x_1(0) = x_2(0) = 0$), both w_1 and x_1 initially increase. When w_1 becomes sufficiently larger than w_2, Eqs. (11a) and (11b) can be approximated as follows:

$$\dot{w}_1 = w_1(1 - \lambda - x_1), \tag{17a}$$

$$\dot{x}_1 = w_1(q_1 - x_1), \tag{17b}$$

since $1 + \frac{w_2}{w_1}$ in Eq. (11b) can be regarded as 1. Note that this system (17) is qualitatively the same as the system (3). According to the same discussion in Sec. III, since we assume the inequality (8), x_1 can exceed $1 - \lambda$ and, thus, w_1 begins to decrease [the same scenario as in Fig. 1(c)]. When w_1 becomes sufficiently small such that $\dot{x}$ in Eq. (11b) becomes negative, x_1 starts to decrease, and w_1 again begins to increase when $x_1 < 1 - \lambda$. We consider that these cycles of alternating increases and decreases, which are analogous to repeated immune response and viral escape from it, are the mechanism behind the damped oscillation.

By applying the same analysis for the case of three viral mutants (i.e., $n = 3$), we also find that oscillatory viral dynamics and synchronized replication rates are observed if one viral mutant has a considerably lower replication rate than the others and its initial value is sufficiently small. See Appendix A for more details about the three viral mutants case.

We generalize these results for n mutants case in which one mutant has a considerably lower replication rate than the others.

V. GENERAL CASE

We consider the system (2) for the general case of n mutants. Let Λ be a real number. By introducing new variables $w_i := v_i e^{-\Lambda t}$, we transform Eq. (2) into the following $2n$-dimensional nonautonomous system:

$$\dot{w}_i = \alpha_i w_i \left(1 - \frac{\Lambda}{\alpha_i} - x_i\right), \tag{18a}$$

$$\dot{x}_i = e^{\Lambda t} w_i \left(q_i - x_i \frac{\sum_{l=1}^n w_l}{w_i}\right), \tag{18b}$$

for $1 \le i \le n$. As in the case when $n = 2$, we are particularly concerned with the situation in which one of the agents v_i has a considerably lower growth rate than the others. Thus, we treat α_n as a small parameter and put $\varepsilon := \alpha_n$. The other parameters are assumed to be $O(1)$.

Definition 1. *We define an internal fixed point as a fixed point whose coordinates are all positive.*

First, we determine Λ so that the system (18) has an internal fixed point.

Theorem 1. *The system (18) has at least one internal fixed point if and only if the following two conditions hold:*

$$\Lambda = \frac{\left(\sum_{l=1}^n \frac{1}{q_l}\right) - 1}{\sum_{l=1}^n \frac{1}{\alpha_l q_l}}, \tag{19}$$

$$\varepsilon \sum_{l=1}^n \frac{1}{\alpha_l q_l} > \left(\sum_{l=1}^n \frac{1}{q_l}\right) - 1. \tag{20}$$

Proof of necessity. Let $(w_i^\dagger, x_i^\dagger)$ with $w_i^\dagger > 0$ and $x_i^\dagger > 0$ be the internal fixed point of system (18). Then, $(w_i^\dagger, x_i^\dagger)$ satisfies

$$x_i^\dagger = 1 - \frac{\Lambda}{\alpha_i} \tag{21}$$

and

$$w_i^\dagger q_i - x_i^\dagger \sum_{l=1}^n w_l^\dagger = 0. \tag{22}$$

We rewrite Eq. (22) as

$$Q_n \boldsymbol{w}^\dagger = \boldsymbol{0}_n, \tag{23}$$

where Q_n is the coefficient matrix given as

$$Q_n := \begin{pmatrix} q_1 - x_1^\dagger & -x_1^\dagger & -x_1^\dagger & \cdots & -x_1^\dagger \\ -x_2^\dagger & q_2 - x_2^\dagger & -x_2^\dagger & \cdots & -x_2^\dagger \\ \vdots & \vdots & \vdots & & \vdots \\ -x_n^\dagger & -x_n^\dagger & -x_n^\dagger & \cdots & q_n - x_n^\dagger \end{pmatrix}, \tag{24}$$

$\boldsymbol{w}^\dagger := {}^t(w_1^\dagger, w_2^\dagger, \ldots, w_n^\dagger)$, and $\boldsymbol{0}_n$ denotes the zero vector of order n. Since we assume $\boldsymbol{w}^\dagger \neq \boldsymbol{0}_n$, Eq. (23) has a nontrivial solution; i.e.,

$$\det Q_n = 0. \tag{25}$$

Lemma 1. *The determinant of the matrix Q_n given in Eq. (24) is calculated as*

$$\det Q_n = \left(1 - \sum_{l=1}^n \frac{x_l^\dagger}{q_l}\right) \prod_{k=1}^n q_k. \tag{26}$$

Proof of Lemma 1. We prove this by induction on n. Obviously, Eq. (26) holds when $n = 2$. We assume that Eq. (26) is true when $n = m$. Then,

$$\det Q_{m+1} = \begin{vmatrix} q_1 - x_1^\dagger & -x_1^\dagger & \cdots & -x_1^\dagger & -x_1^\dagger \\ -x_2^\dagger & q_2 - x_2^\dagger & \cdots & -x_2^\dagger & -x_2^\dagger \\ \vdots & \vdots & & \vdots & \vdots \\ -x_m^\dagger & -x_m^\dagger & \cdots & q_m - x_m^\dagger & -x_m^\dagger \\ -x_{m+1}^\dagger & -x_{m+1}^\dagger & \cdots & -x_{m+1}^\dagger & q_{m+1} - x_{m+1}^\dagger \end{vmatrix}$$

$$= \begin{vmatrix} q_1 - x_1^\dagger & -x_1^\dagger & \cdots & -x_1^\dagger & 0 \\ -x_2^\dagger & q_2 - x_2^\dagger & \cdots & -x_2^\dagger & 0 \\ \vdots & \vdots & & \vdots & \vdots \\ -x_m^\dagger & -x_m^\dagger & \cdots & q_m - x_m^\dagger & 0 \\ -x_{m+1}^\dagger & -x_{m+1}^\dagger & \cdots & -x_{m+1}^\dagger & q_{m+1} \end{vmatrix} + \begin{vmatrix} q_1 - x_1^\dagger & -x_1^\dagger & \cdots & -x_1^\dagger & -x_1^\dagger \\ -x_2^\dagger & q_2 - x_2^\dagger & \cdots & -x_2^\dagger & -x_2^\dagger \\ \vdots & \vdots & & \vdots & \vdots \\ -x_m^\dagger & -x_m^\dagger & \cdots & q_m - x_m^\dagger & -x_m^\dagger \\ -x_{m+1}^\dagger & -x_{m+1}^\dagger & \cdots & -x_{m+1}^\dagger & -x_{m+1}^\dagger \end{vmatrix}$$

$$= q_{m+1} \det Q_m + \begin{vmatrix} q_1 & 0 & \cdots & 0 & -x_1^\dagger \\ & q_2 & \cdots & 0 & -x_2^\dagger \\ & & \ddots & \vdots & \vdots \\ & & & q_m & -x_m^\dagger \\ \mathbf{0} & & & & -x_{m+1}^\dagger \end{vmatrix}$$

$$= q_{m+1}\left(1 - \sum_{l=1}^{m} \frac{x_l^\dagger}{q_l}\right)\left(\prod_{k=1}^{m} q_k\right) - q_1 q_2 \cdots q_m x_{m+1}^\dagger = \left(1 - \sum_{l=1}^{m+1} \frac{x_l^\dagger}{q_l}\right)\prod_{k=1}^{m+1} q_k.$$

□

It, thus, follows from Eq. (25) and Lemma 1 that

$$1 - \sum_{l=1}^{n} \frac{x_l^\dagger}{q_l} = 0. \tag{27}$$

By substituting Eq. (21) into Eq. (27), we obtain Eq. (19). Moreover, since we assume $x_n^\dagger = 1 - \frac{\Lambda}{\varepsilon} > 0$, the inequality (20) follows from Eq. (19).

Proof of sufficiency. We set $x_i^\dagger := 1 - \frac{\Lambda}{\alpha_i}$. Since $\det Q_n = 0$ follows from Eq. (19), Eq. (23) has a nontrivial solution, denoted by $\boldsymbol{w}^\dagger := {}^t(w_1^\dagger, w_2^\dagger, \ldots, w_n^\dagger) \neq \mathbf{0}_n$. Note that $w_i^\dagger$ satisfy Eq. (22). Recall the inequality $\alpha_1 \geq \alpha_2 \geq \cdots \geq \alpha_{n-1} \gg \alpha_n$; we have $x_1^\dagger \geq x_2^\dagger \geq \cdots \geq x_{n-1}^\dagger > x_n^\dagger$ from $x_i^\dagger := 1 - \frac{\Lambda}{\alpha_i}$. Hence, the inequality (20), which is equivalent to $x_n^\dagger > 0$, implies that $x_i^\dagger > 0$ for all i. It, thus, follows from Eq. (22) and $q_i > 0$ that each $w_i^\dagger$ has the same sign with $\sum_{l=1}^{n} w_l^\dagger$. Then, all $w_i^\dagger$ have the same sign, i.e, $w_i^\dagger > 0$ for all i or $w_i^\dagger < 0$ for all i. If $w_i^\dagger < 0$ for all i, then $(x_i^\dagger, -w_i^\dagger)$ is an internal fixed point of system (18) because $-\boldsymbol{w}^\dagger = {}^t(-w_1^\dagger, -w_2^\dagger, \ldots, -w_n^\dagger)$ is also a nontrivial solution of Eq. (23). Hence, the system (18) has at least one internal fixed point.

Thus, we have shown Theorem 1. □

In the following discussion, we set Λ as Eq. (19) and assume the inequality (20). We also assume

$$\sum_{l=1}^{n} \frac{1}{q_l} > 1, \tag{28}$$

so that $\Lambda > 0$. It follows from Eq. (19) and the assumption $\varepsilon \ll 1$ that

$$\Lambda = \frac{\varepsilon\left[\left(\sum_{l=1}^{n} \frac{1}{q_l}\right) - 1\right]}{\frac{1}{q_n} + \varepsilon \sum_{l=1}^{n-1} \frac{1}{\alpha_l q_l}} = O(\varepsilon). \tag{29}$$

Next, we perform the stability analysis assuming timescale separation. As far as $t = O(1)$, we can safely replace $e^{\Lambda t}$ in Eq. (18b) with 1 because $e^{\Lambda t} = 1 + O(\Lambda t) = 1 + O(\varepsilon)$. We also see that w_n is a slow variable and $w_1, \ldots, w_{n-1}, x_1, \ldots, x_{n-1}$, and x_n are fast variables. Thus, in a good approximation, the dynamics of these fast variables are described by the following $(2n-1)$-dimensional autonomous subsystem:

$$\dot{w}_j = \alpha_j w_j \left(1 - \frac{\Lambda}{\alpha_j} - x_j\right), \tag{30a}$$

$$\dot{x}_i = w_i \left(q_i - x_i \frac{\sum_{l=1}^{n} w_l}{w_i}\right), \tag{30b}$$

for $1 \leq j \leq n-1$ and $1 \leq i \leq n$. Note that w_n is regarded as a constant. □

Theorem 2. *The subsystem (30) has the unique internal fixed point (w_j^*, x_i^*) whose coordinates are given as*

$$x_i^* = 1 - \frac{\Lambda}{\alpha_i}, \tag{31}$$

for $1 \le i \le n$ *and*

$$\begin{pmatrix} w_1^* \\ w_2^* \\ \vdots \\ w_{n-1}^* \end{pmatrix} = w_n R^{-1} \begin{pmatrix} x_1^* \\ x_2^* \\ \vdots \\ x_{n-1}^* \end{pmatrix}, \tag{32}$$

where R *is a regular matrix written as*

$$R := \begin{pmatrix} q_1 - x_1^* & -x_1^* & \cdots & -x_1^* \\ -x_2^* & q_2 - x_2^* & \cdots & -x_2^* \\ \vdots & \vdots & & \vdots \\ -x_{n-1}^* & -x_{n-1}^* & \cdots & q_{n-1} - x_{n-1}^* \end{pmatrix}. \tag{33}$$

Proof. Let us assume the existence of an internal fixed point (w_j^*, x_i^*) of the subsystem (30). Then,

$$x_j^* = 1 - \frac{\Lambda}{\alpha_j}, \tag{34}$$

$$w_j^* q_j - x_j^* \left(w_n + \sum_{l=1}^{n-1} w_l^* \right) = 0, \tag{35}$$

for $1 \le j \le n-1$ and

$$w_n q_n - x_n^* \left(w_n + \sum_{l=1}^{n-1} w_l^* \right) = 0. \tag{36}$$

Equation (35) can be rewritten as

$$R \begin{pmatrix} w_1^* \\ w_2^* \\ \vdots \\ w_{n-1}^* \end{pmatrix} = w_n \begin{pmatrix} x_1^* \\ x_2^* \\ \vdots \\ x_{n-1}^* \end{pmatrix}, \tag{37}$$

where R is given in Eq. (33). According to Lemma 1,

$$\det R = \left(1 - \sum_{l=1}^{n-1} \frac{x_l^*}{q_l} \right) \prod_{k=1}^{n-1} q_k. \tag{38}$$

Note that

$$1 - \sum_{l=1}^{n-1} \frac{x_l^*}{q_l} = \frac{1}{\varepsilon q_n \sum_{l=1}^{n} \frac{1}{\alpha_l q_l}} \left[\varepsilon \sum_{l=1}^{n} \frac{1}{\alpha_l q_l} - \left(\sum_{l=1}^{n} \frac{1}{q_l} \right) + 1 \right] > 0 \tag{39}$$

follows from Eqs. (19) and (34), and inequality (20). Thus, R is a regular matrix, which implies that Eq. (37) can be solved as

$$\begin{pmatrix} w_1^* \\ w_2^* \\ \vdots \\ w_{n-1}^* \end{pmatrix} = w_n R^{-1} \begin{pmatrix} x_1^* \\ x_2^* \\ \vdots \\ x_{n-1}^* \end{pmatrix}. \tag{40}$$

By dividing both sides of Eq. (35) by q_j and summing from $j = 1$ to $n-1$, we obtain

$$\sum_{l=1}^{n-1} w_l^* = \frac{w_n \sum_{j=1}^{n-1} \frac{x_j^*}{q_j}}{1 - \sum_{j=1}^{n-1} \frac{x_j^*}{q_j}}. \tag{41}$$

Substituting Eq. (41) into Eq. (36), we have

$$x_n^* = q_n \left(1 - \sum_{j=1}^{n-1} \frac{x_j^*}{q_j} \right) = 1 - \frac{\Lambda}{\alpha_n}. \tag{42}$$

Obviously,

$$x_1^* \ge x_2^* \ge \cdots \ge x_{n-1}^* > x_n^* > 0, \tag{43}$$

from $\alpha_1 \ge \alpha_2 \ge \cdots \ge \alpha_{n-1} \gg \alpha_n$ and inequality (39). It also follows from inequalities (39), (43), and Eq. (41) that $\sum_{l=1}^{n-1} w_l^* > 0$, which implies that $w_j^* > 0$ for $1 \le j \le n-1$ from Eq. (35). Therefore, we have shown that the point (w_j^*, x_i^*) given by Eqs. (31) and (32) is the unique internal fixed point of the subsystem (30). □

Remark 1. *Obviously,* x_i^* *and* $\frac{w_j^*}{w_n}$ *are independent of* w_n.

Let J be the Jacobian matrix at the fixed point (w_j^*, x_i^*) of system (30). Then,

$$J = \begin{pmatrix} O_{n-1,n-1} & A & \mathbf{0}_{n-1} \\ R & B & \mathbf{0}_{n-1} \\ {}^t\boldsymbol{x_n^*} & {}^t\mathbf{0}_{n-1} & -bw_n \end{pmatrix}, \tag{44}$$

where

$$A := -w_n \mathrm{diag}(a_1, a_2, \ldots, a_{n-1}), \quad B := -bw_n I_{n-1},$$
$${}^t\boldsymbol{x_n^*} := -\begin{pmatrix} x_n^* & x_n^* & \cdots & x_n^* \end{pmatrix},$$
$$a_j := \frac{\alpha_j w_j^*}{w_n}, b := \frac{(\sum_{l=1}^{n-1} w_l^*) + w_n}{w_n}.$$

Here, $O_{m,n}$ denotes the $m \times n$ zero matrix, and I_{n-1} is the identity matrix of order $n-1$. Note that a_j and b do not depend on w_n. Our purpose is to show that (i) the fixed point (w_j^*, x_i^*) is asymptotically stable and (ii) damped oscillation occurs if w_n is sufficiently small. In other words, we are going to prove the next theorem:

Theorem 3.

(1) *The real parts of the eigenvalues of the Jacobian matrix J are all negative.*
(2) *There exists a positive constant W such that J has at least one imaginary eigenvalue if and only if* $0 < w_n < W$.

Proof. Let $f(z) := \det(zI_{2n-1} - J)$ be the characteristic polynomial of J. Then,

$$f(z) = (z + bw_n) \det \begin{pmatrix} zI_{n-1} & -A \\ -R & (z + bw_n) I_{n-1} \end{pmatrix}. \tag{45}$$

Recall the next formula;[16] if S, T, U, V are square matrices and if $SU = US$, then

$$\det \begin{pmatrix} S & T \\ U & V \end{pmatrix} = \det(SV - UT). \tag{46}$$

We have

$$\det\begin{pmatrix} zI_{n-1} & -A \\ -R & (z+bw_n)I_{n-1}\end{pmatrix}$$

$$= \left| z(z+bw_n)I_{n-1} - w_n \begin{pmatrix} a_1(x_1^*-q_1) & a_2x_1^* & \cdots & a_{n-2}x_1^* & a_{n-1}x_1^* \\ a_1x_2^* & a_2(x_2^*-q_2) & \cdots & a_{n-2}x_2^* & a_{n-1}x_2^* \\ \vdots & \vdots & & \vdots & \vdots \\ a_1x_{n-2}^* & a_2x_{n-2}^* & \cdots & a_{n-2}(x_{n-2}^*-q_{n-2}) & a_{n-1}x_{n-2}^* \\ a_1x_{n-1}^* & a_2x_{n-1}^* & \cdots & a_{n-2}x_{n-1}^* & a_{n-1}(x_{n-1}^*-q_{n-1}) \end{pmatrix} \right|$$

$$= \begin{vmatrix} z^2+bw_nz+w_na_1(q_1-x_1^*) & -w_na_2x_1^* & \cdots & -w_na_{n-2}x_1^* & -w_na_{n-1}x_1^* \\ -w_na_1x_2^* & z^2+bw_nz+w_na_2(q_2-x_2^*) & \cdots & -w_na_{n-2}x_2^* & -w_na_{n-1}x_2^* \\ \vdots & \vdots & & \vdots & \vdots \\ -w_na_1x_{n-2}^* & -w_na_2x_{n-2}^* & \cdots & z^2+bw_nz+w_na_{n-2}(q_{n-2}-x_{n-2}^*) & -w_na_{n-1}x_{n-2}^* \\ -w_na_1x_{n-1}^* & -w_na_2x_{n-1}^* & \cdots & -w_na_{n-2}x_{n-1}^* & z^2+bw_nz+w_na_{n-1}(q_{n-1}-x_{n-1}^*) \end{vmatrix}$$

$$= \left(\prod_{k=1}^{n-1} a_k\right) \begin{vmatrix} \frac{z^2+bw_nz}{a_1}+w_nq_1-w_nx_1^* & -w_nx_1^* & \cdots & -w_nx_1^* & -w_nx_1^* \\ -w_nx_2^* & \frac{z^2+bw_nz}{a_2}+w_nq_2-w_nx_2^* & \cdots & -w_nx_2^* & -w_nx_2^* \\ \vdots & \vdots & & \vdots & \vdots \\ -w_nx_{n-2}^* & -w_nx_{n-2}^* & \cdots & \frac{z^2+bw_nz}{a_{n-2}}+w_nq_{n-2}-w_nx_{n-2}^* & -w_nx_{n-2}^* \\ -w_nx_{n-1}^* & -w_nx_{n-1}^* & \cdots & -w_nx_{n-1}^* & \frac{z^2+bw_nz}{a_{n-1}}+w_nq_{n-1}-w_nx_{n-1}^* \end{vmatrix}.$$

By replacing $q_k \to (\frac{z^2+bw_nz}{a_k}+w_nq_k)$ and $x_k^\dagger \to w_nx_k^*$ in Lemma. 1, we see that

$$\det\begin{pmatrix} zI_{n-1} & -A \\ -R & (z+bw_n)I_{n-1}\end{pmatrix} = \left(\prod_{k=1}^{n-1} a_k\right)\left(1-\sum_{l=1}^{n-1}\frac{w_nx_l^*}{\frac{z^2+bw_nz}{a_l}+w_nq_l}\right)\prod_{k=1}^{n-1}\left(\frac{z^2+bw_nz}{a_k}+w_nq_k\right)$$

$$= \left(1-\sum_{l=1}^{n-1}\frac{a_lx_l^*w_n}{z^2+bw_nz+a_lq_lw_n}\right)\prod_{k=1}^{n-1}\left(z^2+bw_nz+a_kq_kw_n\right).$$

This implies that

$$f(z) = (z+bw_n)\left(1-\sum_{l=1}^{n-1}\frac{a_lx_l^*w_n}{z^2+bw_nz+a_lq_lw_n}\right) \times \prod_{k=1}^{n-1}\left(z^2+bw_nz+a_kq_kw_n\right). \tag{47}$$

We introduce a new variable X and function $g(X)$ given as

$$X := \frac{z^2+bw_nz}{w_n} \tag{48}$$

and

$$g(X) := \left(1-\sum_{l=1}^{n-1}\frac{a_lx_l^*}{X+a_lq_l}\right)\prod_{k=1}^{n-1}\left(X+a_kq_k\right). \tag{49}$$

It, thus, follows from Eq. (47) that

$$f(z) = (w_n)^{n-1}(z+bw_n)g(X). \tag{50}$$

Note that $g(X)$ is a polynomial of degree $n-1$.

Lemma 2. *The solutions of $g(X)=0$ are all negative real numbers.*

Proof of Lemma 2. We rewrite $g(X)$ as

$$g(X) = \left(1-\sum_{j=1}^{m}\frac{\eta_j}{X+\delta_j}\right)\prod_{i=1}^{m}(X+\delta_i)^{\theta_i}, \tag{51}$$

where δ_i, η_i, and θ_i satisfy the following conditions for $1 \le i \le m$:

$$\prod_{k=1}^{n-1}\left(X+a_kq_k\right) = \prod_{i=1}^{m}(X+\delta_i)^{\theta_i},$$

$$\delta_k < \delta_l \quad \text{if} \quad k < l,$$

and

$$\sum_{l=1}^{n-1}\frac{a_lx_l^*}{X+a_lq_l} = \sum_{j=1}^{m}\frac{\eta_j}{X+\delta_j}.$$

Note that $\delta_i > 0, \eta_i > 0, \theta_i \in \mathbf{N}$, and $\sum_{i=1}^{m} \theta_i = n-1$. We introduce a new function $h(X)$, which is a polynomial of degree m, as

$$h(X) := \left(1 - \sum_{j=1}^{m} \frac{\eta_j}{X+\delta_j}\right) \prod_{i=1}^{m} (X+\delta_i).$$

It follows from Eq. (51) that

$$g(X) = h(X) \prod_{i=1}^{m} (X+\delta_i)^{\theta_i - 1}. \tag{52}$$

By using Eq. (49) and inequality (39), we get

$$g(0) = \left(1 - \sum_{l=1}^{n-1} \frac{x_l^*}{q_l}\right) \prod_{k=1}^{n-1} (a_k q_k) > 0.$$

Thus, $h(0) > 0$ follows from Eq. (52). We also have

$$h(-\delta_i) = -\eta_i \frac{\prod_{i=1}^{m} (X+\delta_i)}{X+\delta_i}\bigg|_{X=-\delta_i}.$$

It follows from $\eta_i > 0$ that

$$\operatorname{sgn} h(-\delta_i) = (-1)^i.$$

We put $\delta_0 := 0$. Then, by the intermediate value theorem, $h(X)$ has a root in each interval $(-\delta_i, -\delta_{i-1})$ for $1 \le i \le m$. Therefore, $h(X)$ has m negative roots. From Eq. (52), we have shown that the roots of $g(X)$ are all negative real numbers. □

According to Lemma 2, there exist positive real numbers ξ_k $(1 \le k \le n-1)$ such that $\xi_1 \le \xi_2 \le \cdots \le \xi_{n-1}$ and

$$g(X) = \prod_{k=1}^{n-1} (X + \xi_k). \tag{53}$$

Since a_k and x_l^* in Eq. (49) do not depend on w_n, $-\xi_k$ [i.e., the solutions of $g(X) = 0$] are independent of w_n. Substituting Eqs. (48) and (53) into Eq. (50), we have

$$f(z) = (z + b w_n) \prod_{k=1}^{n-1} (z^2 + b w_n z + \xi_k w_n). \tag{54}$$

It follows from $b w_n > 0$ and $\xi_k w_n > 0$ that the real parts of the solutions of $f(z) = 0$ are all negative. Thus, the fixed point (w_j^*, x_i^*) is asymptotically stable. We also see that the Jacobian matrix J has at least one imaginary eigenvalue if and only if

$$0 < w_n < \frac{4\xi_{n-1}}{b^2}. \tag{55}$$

Hence, we have proved Theorem 3. □

Based on the same argument as in Sec. IV, the dynamics of slow variable w_n is obtained as $\dot{w}_n = O(\varepsilon^2)$, which implies that $w_n(t) = w_n(0) + O(\varepsilon^2)$ for $t = O(1)$. Thus, from inequality (55), we conclude that oscillation occurs if

$$v_n(0) = w_n(0) < \frac{4\xi_{n-1}}{b^2}. \tag{56}$$

In summary, assuming a few parameter conditions [i.e., the inequalities (20) and (28)], we have shown that (i) all viral mutants have a shared effective growth rate $\Lambda = O(\varepsilon)$ if one mutant has a considerably lower replication rate ε than the others and (ii) oscillatory viral dynamics occur if the initial value of the slowest-replicating mutant is sufficiently small. These findings are the generalization of those obtained in Sec. IV.

VI. DISCUSSION AND CONCLUSION

By performing the linear stability analysis, we find that all growth rates can synchronize to the same value that is as small as the slowest-growing agent [i.e., $O(\varepsilon)$] in the previously proposed mathematical model.[11] This explains the slow exponential growth observed in numerical simulations.[11] We also determine that the oscillatory dynamics appear when the initial value of the slowest-growing agent is sufficiently small.

The inequality (28) represents the same result as in the previous studies[11,17] and it is the parameter condition in which the total viral load eventually diverges. Our study reveals that this condition is valid even without assuming the fast dynamics of immune cells. We also find that the inequality (20) is the condition for the synchronization of all mutants' replication rates. Obviously, the following inequality

$$\sum_{l=1}^{n-1} \frac{1}{q_l} < 1 \tag{57}$$

is a sufficient condition for the inequality (20). Note that the parameter $1/q_i (:= \frac{r_i u}{p_i k})$ characterizes the strength of the ith viral mutant compared with immunity. Then, the inequality (57) suggests that synchronized replication rates are observed when the total virulence of $v_1, \ldots, v_{n-2}$, and v_{n-1} is insufficiently high to cause viral load divergence.

The model we use in this paper was originally proposed as a model of human immunodeficiency virus (HIV).[11] Indeed, this model is consistent with a part of the virological features of HIV; e.g., HIV infects and destroys immune cells,[18,19] HIV produces numerous mutants in the body,[20] and various viral mutants may have different virulence,[21] which is represented by r_i and p_i in this model. However, this model has not been used to study HIV infection in recent years because the model is considered to be not biologically accurate to describe viral dynamics *in vivo*: this model does not incorporate the uninfected target cell population, which is included in the standard HIV infection model.[22]

In the later studies, Nowak and Bangham proposed another model that considers both the uninfected target cell and viral mutation[23] and Iwami *et al.* performed the linear stability analysis of this model for the case of one viral mutant with an assumption that viral dynamics are sufficiently fast.[13] Thus, applying our method to the Nowak and Bangham model is future work.

There are several other possible extensions in our study. We transformed the nonautonomous system (18) into the autonomous one (30) by the approximation that $e^{\Lambda t} \simeq 1$ and assuming timescale separation. These are appropriate approximations because as far as $t = O(1)$, $e^{\Lambda t}$ and the slow variable w_n stay ε-vicinity of 1 and $w_n(0)$, respectively. However, developing a more mathematically rigorous

approach that is valid even when t is sufficiently large, if any, is a future challenge.

The existence of multistability is another open question in this study. Obviously, $v_i = 0$ with arbitrary $x_i \in \mathbf{R}$ is a set of fixed points of the system (2). Furthermore, if the parameters q_i satisfy $\sum_{i=1}^{n}(1/q_i) = 1$, there is another set of fixed points (v_i^*, x_i^*) with $x_i^* = 1$ and $\frac{v_i^*}{\sum_{j=1}^{n} v_j^*} = 1/q_i$. As we discuss in Appendix B for the case when $n = 2$, the qualitatively different solutions, including these fixed points and the diverging solution, can be obtained by using the same parameter but different initial conditions. Thus, we conclude that the system (2) is a multistable system. However, these arguments do not exclude the existence of other dynamics, such as limit cycles or chaos, in the system (2), even though no such behavior was observed in numerical simulation as far as we used different sets of parameter values and initial conditions in the case when $n = 2, 3$. Investigating the detailed structure of the phase plane of the subsystem (30) can be a possible clue to examine the existence of limit cycles and chaos.

Since we mainly analyze the model (2) under the assumption that the growth rate of one viral mutant is sufficiently smaller than the others, elucidating the general behavior of this model without any restrictions on parameters and initial conditions is also a future task. This is a mathematically difficult problem because without assuming $\varepsilon \ll 1$, Λ in Eq. (29) is no longer a small value and, thus, we have to deal with the nonautonomous system (18) instead of the reduced autonomous system (30). Roughly speaking, if all the parameters of viral mutants and immune cells are almost the same (i.e., $\alpha_i \simeq 1$ and $q_i \simeq q$), the system can be approximated to the two-dimensional model (3). Thus, the behavior of the model will roughly become that observed in either Fig. 1(a) (viral load diverges) or Fig. 1(c) (the virus is eradicated). This argument is, needless to say, not sufficient, considering that the parameters of the model can take a wide range of values. The case when the growth rates of multiple viral mutants are sufficiently smaller than the others, or the case when there are significant differences among the parameters of immune strength (i.e., q_i) are important research problems to be clarified.

In conclusion, we analyze in detail the simple mathematical model of asymmetrically interacting agents. We perform linear stability analysis and find the unique features of the model; i.e., the viral load initially oscillates and then slowly increases if the parameters and initial values satisfy a few conditions. Our work also proposes an analytical method of applying stability analysis to the exponentially diverging solution by using the techniques of variable transformation and timescale separation.

ACKNOWLEDGMENTS

This study was initiated by the first-named author at the summer school of iBMath (Institute for Biology and Mathematics of Dynamic Cellular Processes, The University of Tokyo). We thank the former members of iBMath, especially Y. Nakata, H. Kurihara, and T. Tokihiro, for mathematical advice. This study was supported by JSPS KAKENHI (No. JP23KJ0756) to Y.K. and JSPS KAKENHI (No. JP21K12056) to H.K.

AUTHOR DECLARATIONS

Conflict of Interest

The authors have no conflicts to disclose.

Author Contributions

Y.K. initiated this research. H.K. proposed the research direction. Y.K. performed the analysis and numerical simulations. Y.K. wrote the manuscript under the mentorship of H.K.

Yusuke Kato: Conceptualization (lead); Formal analysis (lead); Investigation (lead); Visualization (lead); Writing – original draft (lead). **Hiroshi Kori:** Supervision (lead); Writing – original draft (supporting).

DATA AVAILABILITY

The data that support the findings of this study are available within the article.

APPENDIX A: THE CASE WHEN $n = 3$

We consider the following system:

$$\dot{v}_1 = v_1(1 - x_1), \tag{A1a}$$

$$\dot{v}_2 = \alpha_2 v_2(1 - x_2), \tag{A1b}$$

$$\dot{v}_3 = \alpha_3 v_3(1 - x_3), \tag{A1c}$$

$$\dot{x}_1 = v_1\left[q_1 - x_1\left(1 + \frac{v_2}{v_1} + \frac{v_3}{v_1}\right)\right], \tag{A1d}$$

$$\dot{x}_2 = v_2\left[q_2 - x_2\left(1 + \frac{v_1}{v_2} + \frac{v_3}{v_2}\right)\right], \tag{A1e}$$

$$\dot{x}_3 = v_3\left[q_3 - x_3\left(1 + \frac{v_1}{v_3} + \frac{v_2}{v_3}\right)\right]. \tag{A1f}$$

We treat α_3 as a small parameter (i.e., $\alpha_3 \ll 1$) and put $\varepsilon := \alpha_3$. The other parameters are assumed to be $O(1)$. As in the case of two viral mutants, we introduce new variables $\beta := \frac{v_2}{v_1}$ and $\gamma := \frac{v_3}{v_1}$. Assuming the convergence of β and γ to positive constants β^* and γ^*, respectively, we see that

$$x_1^* = \frac{q_1}{1 + \beta^* + \gamma^*}, \quad x_2^* = \frac{\beta^* q_2}{1 + \beta^* + \gamma^*}, \quad \text{and} \quad x_3^* = \frac{\gamma^* q_3}{1 + \beta^* + \gamma^*}, \tag{A2}$$

are fixed points of the subsystem given by Eqs. (A1d), (A1e), and (A1f). Substituting $x_i = x_i^*$ into the equations $\dot{\beta} = \frac{v_1\dot{v}_2 - v_2\dot{v}_1}{v_1^2} = 0$ and

$\dot{\gamma} = \frac{v_1\dot{v}_3 - v_3\dot{v}_1}{v_1^2} = 0$, we obtain the following:

$$\beta^* = \frac{\alpha_2 q_1 + \varepsilon(q_1q_3 - q_1 - q_3) + \alpha_2\varepsilon q_3}{\alpha_2 q_2 + \varepsilon q_3 + \alpha_2\varepsilon(q_2q_3 - q_2 - q_3)} = \frac{q_1}{q_2} + O(\varepsilon), \tag{A3}$$

and

$$\gamma^* = \frac{\alpha_2(q_1q_2 - q_1 - q_2) + \varepsilon q_1 + \alpha_2\varepsilon q_2}{\alpha_2 q_2 + \varepsilon q_3 + \alpha_2\varepsilon(q_2q_3 - q_2 - q_3)} = \frac{q_1q_2 - q_1 - q_2}{q_2} + O(\varepsilon). \tag{A4}$$

For sufficiently small ε, the conditions $\beta^* > 0$ and $\gamma^* > 0$ hold if

$$q_1q_2 - q_1 - q_2 > 0. \tag{A5}$$

We assume this inequality (A5) for the following argument.

Substituting $x_i = x_i^*$ and $(\beta, \gamma) = (\beta^*, \gamma^*)$ into Eqs. (A1a)–(A1c), we acquire the following equation:

$$\dot{v}_i = \lambda v_i,$$

where

$$\lambda = \frac{\alpha_2\varepsilon(q_1q_2 + q_2q_3 + q_3q_1 - q_1q_2q_3)}{\alpha_2 q_1q_2 + \varepsilon q_3q_1 + \alpha_2\varepsilon q_2q_3} = O(\varepsilon). \tag{A6}$$

We also assume

$$q_1q_2 + q_2q_3 + q_3q_1 - q_1q_2q_3 > 0 \tag{A7}$$

so that $\lambda > 0$.

Next, we perform the linear stability analysis. By introducing new variables $w_i := v_i e^{-\lambda t}$, we transform Eq. (A1) into the following six-dimensional nonautonomous system:

$$\dot{w}_1 = w_1(1 - \lambda - x_1), \tag{A8a}$$

$$\dot{w}_2 = \alpha_2 w_2\left(1 - \frac{\lambda}{\alpha_2} - x_2\right), \tag{A8b}$$

$$\dot{w}_3 = \varepsilon w_3\left(1 - \frac{\lambda}{\varepsilon} - x_3\right), \tag{A8c}$$

$$\dot{x}_1 = e^{\lambda t} w_1\left[q_1 - x_1\left(1 + \frac{w_2}{w_1} + \frac{w_3}{w_1}\right)\right], \tag{A8d}$$

$$\dot{x}_2 = e^{\lambda t} w_2\left[q_2 - x_2\left(1 + \frac{w_1}{w_2} + \frac{w_3}{w_2}\right)\right], \tag{A8e}$$

$$\dot{x}_3 = e^{\lambda t} w_3\left[q_3 - x_3\left(1 + \frac{w_1}{w_3} + \frac{w_2}{w_3}\right)\right]. \tag{A8f}$$

As far as $t = O(1)$, we can safely replace $e^{\lambda t}$ in Eq. (A8) with 1 since $e^{\lambda t} = 1 + O(\lambda t) = 1 + O(\varepsilon)$. Moreover, w_3 is a slow variable and w_1, w_2, x_1, x_2, and x_3 are fast variables. Thus, in a good approximation, the dynamics of these fast variables are described by the five-dimensional autonomous subsystem as below:

$$\dot{w}_1 = w_1(1 - \lambda - x_1), \tag{A9a}$$

$$\dot{w}_2 = \alpha_2 w_2\left(1 - \frac{\lambda}{\alpha_2} - x_2\right), \tag{A9b}$$

$$\dot{x}_1 = w_1\left[q_1 - x_1\left(1 + \frac{w_2}{w_1} + \frac{w_3}{w_1}\right)\right], \tag{A9c}$$

$$\dot{x}_2 = w_2\left[q_2 - x_2\left(1 + \frac{w_1}{w_2} + \frac{w_3}{w_2}\right)\right], \tag{A9d}$$

$$\dot{x}_3 = w_3\left[q_3 - x_3\left(1 + \frac{w_1}{w_3} + \frac{w_2}{w_3}\right)\right], \tag{A9e}$$

in which w_3 is regarded as a constant. The internal fixed point of this subsystem (A9) is

$$(w_1, w_2, x_1, x_2, x_3) = \left(\frac{w_3}{\gamma^*}, \frac{\beta^* w_3}{\gamma^*}, \frac{q_1}{1 + \beta^* + \gamma^*}, \frac{\beta^* q_2}{1 + \beta^* + \gamma^*}, \frac{\gamma^* q_3}{1 + \beta^* + \gamma^*}\right). \tag{A10}$$

The Jacobian matrix at this fixed point is

$$\begin{pmatrix} 0 & 0 & -e_1 & 0 & 0 \\ 0 & 0 & 0 & -e_2 & 0 \\ e_3 & -e_4 & -e_8 & 0 & 0 \\ -e_5 & e_6 & 0 & -e_8 & 0 \\ -e_7 & -e_7 & 0 & 0 & -e_8 \end{pmatrix}, \tag{A11}$$

where $e_1, \ldots, e_8$ are positive constants given by

$$e_1 = \frac{w_3}{\gamma^*}, \quad e_2 = \frac{\alpha_2\beta^* w_3}{\gamma^*}, \quad e_3 = \frac{q_1(\beta^* + \gamma^*)}{1 + \beta^* + \gamma^*},$$
$$e_4 = \frac{q_1}{1 + \beta^* + \gamma^*}, \quad e_5 = \frac{q_2\beta^*}{1 + \beta^* + \gamma^*}, \quad e_6 = \frac{q_2(1 + \gamma^*)}{1 + \beta^* + \gamma^*}, \tag{A12}$$
$$e_7 = \frac{q_3\gamma^*}{1 + \beta^* + \gamma^*}, \quad \text{and} \quad e_8 = \frac{(1 + \beta^* + \gamma^*)w_3}{\gamma^*}.$$

The eigenvalues of matrix (A11) are

$$-e_8, \quad -\frac{e_8}{2} + \frac{1}{2}\sqrt{e_8^2 - 2(e_1e_3 + e_2e_6) \pm 2\sqrt{(e_1e_3 - e_2e_6)^2 + 4e_1e_2e_4e_5}},$$

and

$$-\frac{e_8}{2} - \frac{1}{2}\sqrt{e_8^2 - 2(e_1e_3 + e_2e_6) \pm 2\sqrt{(e_1e_3 - e_2e_6)^2 + 4e_1e_2e_4e_5}}. \tag{A13}$$

From $e_3e_6 > e_4e_5$, we conclude that the real parts of these eigenvalues are all negative, which implies that the fixed point (A10) is asymptotically stable. Moreover, imaginary eigenvalues appear if

$$e_8^2 - 2(e_1e_3 + e_2e_6) - 2\sqrt{(e_1e_3 - e_2e_6)^2 + 4e_1e_2e_4e_5} < 0. \tag{A14}$$

Substituting Eq. (A12) into inequality (A14), we have

$$w_3^2\left(\frac{1+\beta^*+\gamma^*}{\gamma^*}\right)^2 - 2w_3\left\{\frac{q_1(\beta^*+\gamma^*)+\alpha_2q_2\beta^*(1+\gamma^*)+\sqrt{[q_1(\beta^*+\gamma^*)-\alpha_2q_2\beta^*(1+\gamma^*)]^2+4\alpha_2q_1q_2(\beta^*)^2}}{\gamma^*(1+\beta^*+\gamma^*)}\right\} < 0$$

$$\iff 0 < w_3 < \frac{2\gamma^*\left\{q_1(\beta^*+\gamma^*)+\alpha_2q_2\beta^*(1+\gamma^*)+\sqrt{[q_1(\beta^*+\gamma^*)-\alpha_2q_2\beta^*(1+\gamma^*)]^2+4\alpha_2q_1q_2(\beta^*)^2}\right\}}{(1+\beta^*+\gamma^*)^3}. \tag{A15}$$

The fast variables stay in the ε-vicinity of the fixed point in the full system after the transient process because the subsystem of the fast variables has the stable fixed point (A10). Substituting $x_3 = x_3^* + O(\varepsilon)$ into Eq. (A8c) and further using Eqs. (A3), (A4), and (A6), we obtain $\dot{w}_3 = O(\varepsilon^2)$, which implies that $w_3(t) = w_3(0) + O(\varepsilon^2)$ for $t = O(1)$. Therefore, w_3 in inequality (A15) can be regarded as $w_3(0)$ in a good approximation. Thus, we conclude that oscillatory viral dynamics occur if there is a viral strain whose replication rate is considerably lower than the others and its initial value is sufficiently small. We also find that all viral mutants have the following shared effective growth rate: $\lambda = O(\varepsilon)$. Note that these findings are the same as those obtained in the case of two viral mutants.

Finally, we investigate the dynamics of system (A1) by numerical simulation. Figure 3 shows that the expected two features of the model (i.e., damped oscillation and slow exponential viral growth) are observed with the parameters and initial conditions that satisfy the inequalities (A5), (A7), and (A15). These results confirm the validity of our analysis.

APPENDIX B: MULTISTABILITY OF THE MODEL

We investigate whether the system (2) is multistable, using the case when $n = 2$ [i.e., the system (5)] as an example. Obviously,

$$(v_1, v_2, x_1, x_2) = (0, 0, x_1, x_2), \tag{B1}$$

with arbitrary $x_1, x_2 \in \mathbf{R}$ is a set of fixed points of the system (5). The Jacobian matrix at these fixed points is

$$\begin{pmatrix} 1-x_1 & 0 & -v_1 & 0 \\ 0 & \alpha_2(1-x_2) & 0 & -\alpha_2v_2 \\ q_1-x_1 & -x_1 & -(v_1+v_2) & 0 \\ -x_2 & q_2-x_2 & 0 & -(v_1+v_2) \end{pmatrix}\Bigg|_{(v_1,v_2,x_1,x_2)=(0,0,x_1,x_2)} \tag{B2}$$

$$= \begin{pmatrix} 1-x_1 & 0 & 0 & 0 \\ 0 & \alpha_2(1-x_2) & 0 & 0 \\ q_1-x_1 & -x_1 & 0 & 0 \\ -x_2 & q_2-x_2 & 0 & 0 \end{pmatrix}, \tag{B3}$$

and its eigenvalues are 0, $1 - x_1$, and $1 - x_2$. The 0 eigenvalue corresponds to the eigenvectors ${}^t(0, 0, 1, 0)$ and ${}^t(0, 0, 0, 1)$, which are parallel to the plane $v_1 = v_2 = 0$ (the set of fixed points). Thus, we expect that these fixed points are Lyapunov stable if $x_1 > 1$ and $x_2 > 1$.

Figure 4 shows the numerical simulation results of Eq. (5). In Figs. 4(a) and 4(b), we use the same parameter as in Figs. 2(a) and 2(b) but different initial conditions. In both cases, the system converges to the fixed point (B1). However, the steady-state values of x_i are different between Fig. 2(b) and Fig. 4(b), which implies that the fixed points (B1) are multistable. In Figs. 4(c) and 4(d), we use the same parameter as in Figs. 2(c) and 2(d) but different initial conditions. The system converges to the fixed point (B1) in Figs. 4(c) and 4(d), while the viral load diverges in Figs. 2(c) and 2(d).

The system (5) has another set of fixed points

$$(v_1, v_2, x_1, x_2) = (v_1, (q_1 - 1)v_1, 1, 1), \tag{B4}$$

with arbitrary $v_1 \in \mathbf{R}$ if the parameters q_i satisfy

$$\frac{1}{q_1} + \frac{1}{q_2} = 1. \tag{B5}$$

Noting that $q_2 = \frac{q_1}{q_1-1}$, the Jacobian matrix at these fixed points is

$$\begin{pmatrix} 0 & 0 & -v_1 & 0 \\ 0 & 0 & 0 & -\alpha_2(q_1-1)v_1 \\ q_1-1 & -1 & -q_1v_1 & 0 \\ -1 & \frac{1}{q_1-1} & 0 & -q_1v_1 \end{pmatrix}, \tag{B6}$$

and its eigenvalues are

$$0, \quad -q_1v_1, \quad \text{and} \quad \frac{1}{2}(-q_1v_1 \pm \sqrt{\sigma}), \tag{B7}$$

where

$$\sigma = q_1^2v_1^2 - 4v_1(q_1 + \alpha_2 - 1). \tag{B8}$$

The 0 eigenvalue corresponds to the eigenvector ${}^t(1, q_1 - 1, 0, 0)$, which is parallel to the set of fixed points (B4). Since we assume $q_i > 0$, then $q_1 > 1$ follows from Eq. (B5), which implies that

$$\sigma < q_1^2v_1^2, \tag{B9}$$

and thus the real parts of the eigenvalues $\frac{1}{2}(-q_1v_1 \pm \sqrt{\sigma})$ are negative. Therefore, we expect that the fixed points (B5) are Lyapunov stable.

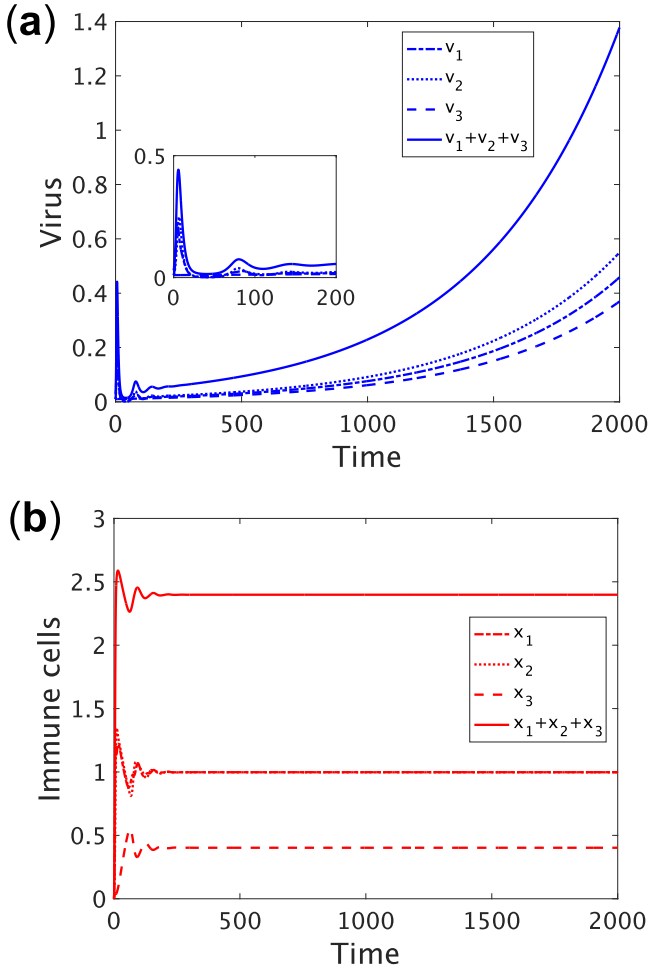

FIG. 3. Numerical simulation results of Eqs. (A1). Panels (a) and (b) show the time course of the viral load and the immune cells, respectively. By choosing the parameters and initial conditions to match the analytical results, the two features (i.e., damped oscillation and slow exponential viral growth) are also reproduced in the case of three viral mutants. The parameters and initial conditions of this simulation are as follows: $\alpha_2 = 0.75, \alpha_3 = 0.003, q_1 = 3.0, q_2 = 2.5, q_3 = 1.5, v_1(0) = v_2(0) = v_3(0) = 0.01, x_1(0) = x_2(0) = x_3(0) = 0$. Note that these values satisfy the inequalities (A5), (A7), and (A15).

Figure 5 shows the simulation results of Eq. (5) under the parameter condition (B5). By changing the initial conditions, the system can converge to the different fixed points, i.e., the fixed point (B1) in Figs. 5(a) and 5(b), and the fixed point (B4) in Figs. 5(c) and 5(d), respectively. Note that the condition (B5) corresponds to $\lambda = 0$ in Eq. (9), which agrees with the viral dynamics in Fig. 5(c) where the viral load neither diverges nor diminishes.

According to the above analysis and numerical simulations, we conclude that the model system (2) is multistable, meaning that qualitatively different solutions, including the fixed points and the diverging solution, can be obtained by using the same parameter but different initial conditions.

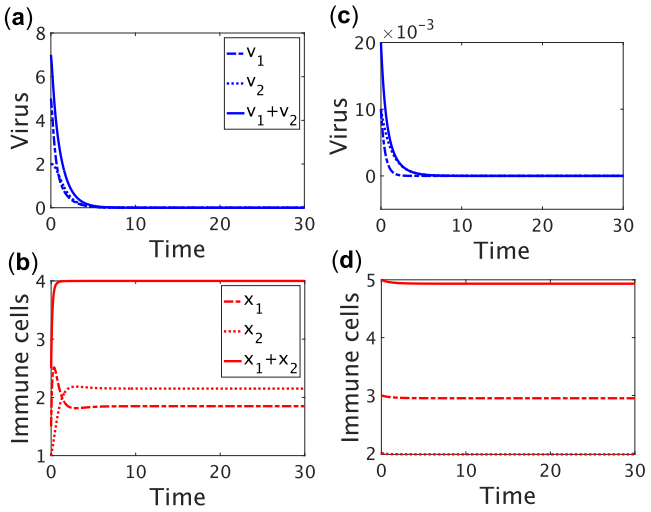

FIG. 4. Numerical simulation results of Eq. (5). In panels (a) and (b), we use the same parameter as in Figs. 2(a) and 2(b) ($\alpha_2 = 0.75, q_1 = q_2 = 4.0$) but different initial conditions $v_1(0) = 5.0, v_2(0) = 2.0, x_1(0) = 1.5, x_2(0) = 1.0$. Even though the system converges to the fixed points (B1) in both Figs. 2(a) and 2(b) and Figs. 4(a) and 4(b), the steady-state values of x_i are different, which implies that the fixed points (B1) are multistable. In panels (c) and (d), we use the same parameter as in Figs. 2(c) and 2(d) ($\alpha_2 = 0.75, q_1 = q_2 = \frac{4}{3}$) but different initial conditions $v_1(0) = v_2(0) = 0.01, x_1(0) = 3.0, x_2(0) = 2.0$. The system converges to the fixed point (B1), while the viral load diverges in Figs. 2(c) and 2(d).

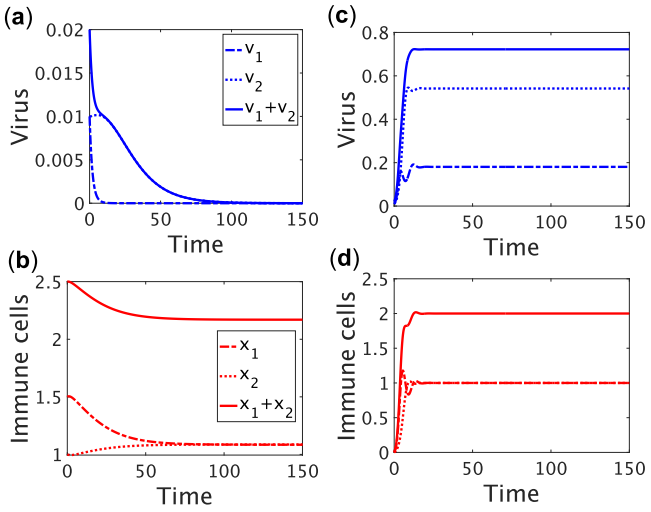

FIG. 5. Numerical simulation results of Eq. (5) when the condition (B5) is satisfied. We use the same parameter but different initial conditions between panels (a) and (b) and panels (c) and (d). The system converges to the fixed point (B1) in (a) and (b), while converging to the fixed point (B4) in (c) and (d). The parameters and initial conditions are as follows: $\alpha_2 = 0.75, q_1 = 4.0, q_2 = 4/3$ for the whole figure, $v_1(0) = 0.01, v_2(0) = 0.01, x_1(0) = 1.5, x_2(0) = 1.0$ for panels (a) and (b), and $v_1(0) = 0.01, v_2(0) = 0.01, x_1(0) = 0, x_2(0) = 0$ for panels (c) and (d).

REFERENCES

[1] S. H. Strogatz, *Nonlinear Dynamics and Chaos* (CRC Press, 2018).
[2] E. N. Lorenz, "Deterministic nonperiodic flow," J. Atmos. Sci. **20**, 130–141 (1963).
[3] A. T. Winfree, "Biological rhythms and the behavior of populations of coupled oscillators," J. Theor. Biol. **16**, 15–42 (1967).
[4] Y. Kuramoto, *Chemical Oscillations, Waves, and Turbulence* (Springer, New York, 1984).
[5] J. D. Murray, *Mathematical Biology: I. An Introduction* (Springer, 2002).
[6] D. Ludwig, D. D. Jones, and C. S. Holling, "Qualitative analysis of insect outbreak systems: The spruce budworm and forest," J. Animal Ecol. **47**, 315–332 (1978).
[7] A. J. Lotka, "Undamped oscillations derived from the law of mass action," J. Am. Chem. Soc. **42**, 1595–1599 (1920).
[8] V. Volterra, "Variations and fluctuations of the number of individuals in animal species living together," ICES J. Mar. Sci. **3**, 3–51 (1928).
[9] R. E. Mirollo and S. H. Strogatz, "Synchronization of pulse-coupled biological oscillators," SIAM J. Appl. Math. **50**, 1645–1662 (1990).
[10] I. Aihara, R. Takeda, T. Mizumoto, T. Otsuka, T. Takahashi, H. G. Okuno, and K. Aihara, "Complex and transitive synchronization in a frustrated system of calling frogs," Phys. Rev. E **83**, 031913 (2011).
[11] M. A. Nowak and R. M. May, "Coexistence and competition in HIV infections," J. Theor. Biol. **159**, 329–342 (1992).
[12] A. Murase, T. Sasaki, and T. Kajiwara, "Stability analysis of pathogen-immune interaction dynamics," J. Math. Biol. **51**, 247–267 (2005).
[13] S. Iwami, S. Nakaoka, and Y. Takeuchi, "Frequency dependence and viral diversity imply chaos in an HIV model," Physica D **223**, 222–228 (2006).
[14] S. Iwami, S. Nakaoka, and Y. Takeuchi, "Mathematical analysis of a HIV model with frequency dependence and viral diversity," Math. Biosci. Eng. **5**, 457 (2008).
[15] W.-M. Liu, "Nonlinear oscillations in models of immune responses to persistent viruses," Theor. Popul. Biol. **52**, 224–230 (1997).
[16] D. Serre, *Matrices: Theory and Applications*, 2nd ed. (Springer, New York, 2010), pp. 40–41, 61.
[17] M. A. Nowak, "The evolutionary dynamics of HIV infections," in *First European Congress of Mathematics, Paris, 6–10 July 1992* (Springer, 1994), pp. 311–326.
[18] P. R. Gorry and P. Ancuta, "Coreceptors and HIV-1 pathogenesis," Curr. HIV/AIDS Rep. **8**, 45–53 (2011).
[19] B. G. Turner and M. F. Summers, "Structural biology of HIV," J. Mol. Biol. **285**, 1–32 (1999).
[20] J. M. Cuevas, R. Geller, R. Garijo, J. López-Aldeguer, and R. Sanjuán, "Extremely high mutation rate of HIV-1 in vivo," PLoS Biol. **13**, e1002251 (2015).
[21] A. Rambaut, D. Posada, K. A. Crandall, and E. C. Holmes, "The causes and consequences of HIV evolution," Nat. Rev. Genet. **5**, 52–61 (2004).
[22] A. S. Perelson and R. M. Ribeiro, "Modeling the within-host dynamics of HIV infection," BMC Biol. **11**, 1–10 (2013).
[23] M. A. Nowak and C. R. Bangham, "Population dynamics of immune responses to persistent viruses," Science **272**, 74–79 (1996).